NEUROPROSTHETICS

Improved control of a prosthetic limb by surgically creating electro-neuromuscular constructs with implanted electrodes

Jan Zbinden[1,2], Paolo Sassu[1,3,4], Enzo Mastinu[1,2,5], Eric J. Earley[1,2,6], Maria Munoz-Novoa[1,7], Rickard Brånemark[8,9,10], Max Ortiz-Catalan[1,2,11]*

Remnant muscles in the residual limb after amputation are the most common source of control signals for prosthetic hands, because myoelectric signals can be generated by the user at will. However, for individuals with amputation higher up the arm, such as an above-elbow (transhumeral) amputation, insufficient muscles remain to generate myoelectric signals to enable control of the lost arm and hand joints, thus making intuitive control of wrist and finger prosthetic joints unattainable. We show that severed nerves can be divided along their fascicles and redistributed to concurrently innervate different types of muscle targets, particularly native denervated muscles and nonvascularized free muscle grafts. We engineered these neuromuscular constructs with implanted electrodes that were accessible via a permanent osseointegrated interface, allowing for bidirectional communication with the prosthesis while also providing direct skeletal attachment. We found that the transferred nerves effectively innervated their new targets as shown by a gradual increase in myoelectric signal strength. This allowed for individual flexion and extension of all five fingers of a prosthetic hand by a patient with a transhumeral amputation. Improved prosthetic function in tasks representative of daily life was also observed. This proof-of-concept study indicates that motor neural commands can be increased by creating electro-neuromuscular constructs using distributed nerve transfers to different muscle targets with implanted electrodes, enabling improved control of a limb prosthesis.

INTRODUCTION

Upper limb amputation substantially changes the way in which one interacts with the environment, with the most proximal amputations suffering from the highest impairment because function decreases with every lost joint. Mechatronic joints can now be combined to replace limbs lost to amputations. However, commanding artificial joints in a similar manner to biological ones has remained challenging. Myoelectric signals extracted from residual muscles in the stump have been the preferred source of control in mechatronic prostheses (myoelectric prostheses). The standard clinical solution is for prosthetic users to modulate the activity of an antagonistic pair of remnant muscles to drive the activation of a single degree-of-freedom (DoF) prosthetic joint. The problem is that there are not enough remnant muscles to drive several prosthetic joints in an intuitive manner. For example, the opening and closing of a prosthetic hand can be driven by the contraction of the biceps and triceps muscles in a transhumeral amputation, but no other muscles are left to control the prosthetic elbow, wrist, or individual fingers.

Surgically reconstructing the extremity can ameliorate the problem of insufficient control signals by creating new myoelectric sites (*1*). Nerve transfers to native but denervated muscles, also known as targeted muscle reinnervation (*2*), have gained popularity in the past decade. This procedure repurposes remnant muscles at the stump to amplify neural motor commands to the missing joints. This is achieved by denervating a muscle with dispensable biomechanical function and then reinnervating it with a major nerve severed by the amputation (i.e., a nerve transfer). Once the muscle has been reinnervated, electrodes on the surface of the skin can be used to record neural commands to the missing limb, because the reinnervated muscles are large enough to radiate electrical signals transcutaneously. A downside of this approach is that all of the motor information normally contained in the severed nerves is reduced to a single myoelectric signal. Therefore, reconstruction with nerve transfers to native muscles has only allowed for up to six independent control signals (*3*), which are enough to drive a mechatronic elbow, wrist, and end effector (each using a pair of signals/electrodes). However, dexterous manipulation of objects is not possible with this approach, because no additional information is left for individual finger control.

Recently, another surgical approach has been suggested in which, rather than transferring the severed nerve to a native muscle, the nerve is longitudinally dissected into several fascicles, and then each fascicle is wrapped with a free muscle graft. This strategy, also known as regenerative peripheral nerve interface (*4*, *5*), aims at extracting more motor neural information at the cost of accessibility. Accessibility here is a problem, because the free muscle grafts are too small to be recorded with surface electrodes, and thus the implementation of such an approach in prosthetic devices requires the use of implanted electrodes (*6*). Implanted electrodes

[1]Center for Bionics and Pain Research, Mölndal, Sweden. [2]Department of Electrical Engineering, Chalmers University of Technology, Gothenburg, Sweden. [3]Department of Hand Surgery, Sahlgrenska University Hospital, Mölndal, Sweden. [4]Department of Orthoplastic, IRCCS Istituto Ortopedico Rizzoli, Bologna, Italy. [5]BioRobotics Institute, Scuola Superiore Sant'Anna, Pisa, Italy. [6]Osseointegration Research Consortium, University of Colorado, Aurora, CO, USA. [7]Center for Advanced Reconstruction of Extremities, Sahlgrenska University Hospital, Mölndal, Sweden. [8]K. Lisa Yang Center for Bionics, Massachusetts Institute of Technology, Cambridge, MA, USA. [9]Department of Orthopaedics, Gothenburg University, Gothenburg, Sweden. [10]Integrum AB, Mölndal, Sweden. [11]Bionics Institute, Melbourne, Australia.
*Corresponding author. Email: maxortizc@outlook.com

have been shown to improve prosthetic control compared with their skin surface noninvasive counterparts (*7*–*9*) but bring an additional obstacle to clinical implementation, namely, the need for a safe, reliable, and long-term stable transcutaneous interface between the implanted electrodes and the prosthesis (*10*). The lack of such an interface has hindered the clinical adoption of implanted electrodes and more refined surgical techniques for artificial limb replacement. In this study, we present a combination of surgical reconstruction procedures combined with a long-term stable neuromusculoskeletal interface that allows for bidirectional communication between electro-neuromuscular constructs and the artificial limb in a patient with a transhumeral amputation (fig. S1).

RESULTS

Surgical procedure and neuromusculoskeletal interface

In a patient with a transhumeral amputation, we transected the neuromas of the three major nerves at the residual limb (median, ulnar, and radial) and then dissected each nerve longitudinally in two groups of fascicles. One group was transferred to reinnervate native muscles that were first denervated. Electrodes were then implanted in these (to be) reinnervated native muscles as well as in the other available unreconstructed muscles. The other group of fascicles was further dissected to expose individual fascicles that were then used to reinnervate free muscle grafts harvested from the lower limb. These grafts each housed an intramuscular electrode. These newly created electro-neuromuscular constructs were used to extract motor commands directed to the missing hand, allowing for the intuitive flexion and extension control of all five fingers of a prosthetic hand (movie S1). In addition, improved prosthetic function while performing tasks normally found in daily life was also observed (movie S2).

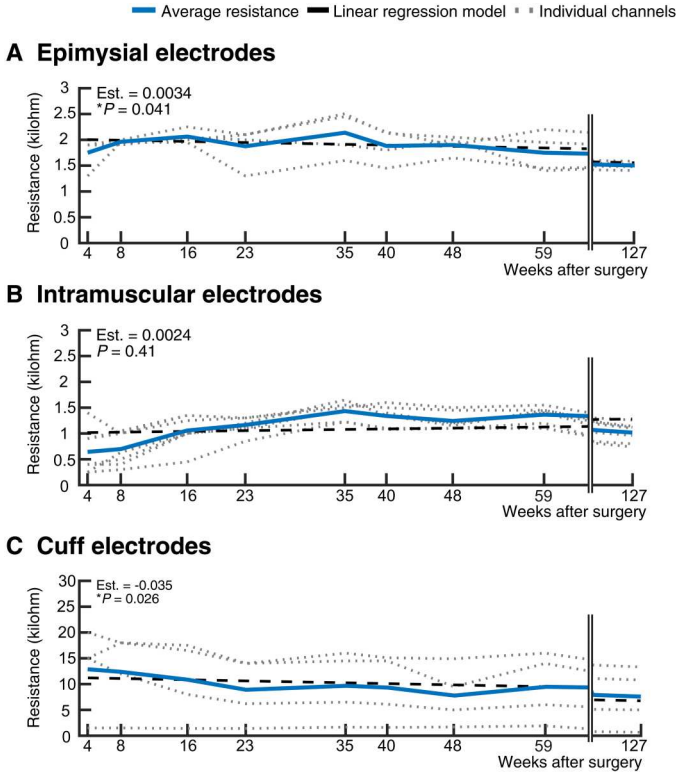

Fig. 1. Electrical resistance of epimysial, intramuscular, and cuff electrodes over time. (**A**) Shown is the electrical resistance of the epimysial electrodes (electrodes sutured to the surface of the muscle) on unreconstructed and reinnervated native muscles in the patient (n = 4 electrodes). (**B**) Shown is the electrical resistance of the intramuscular electrodes in unreconstructed muscles, reinnervated native muscles, and reinnervated free muscle grafts in the patient (n = 8 electrodes). (**C**) Shown is the electrical resistance of the ring contact and three discrete contacts of the cuff electrode surrounding a fascicle of the median nerve (n = 4 cuff electrode contacts).

The 51-year-old male who had lost his left arm above the elbow because of a traumatic injury was initially provided with a conventional myoelectric prosthesis using skin surface electrodes but used it rarely because of discomfort related to the socket attachment. In addition, he was unsatisfied with the limited and unreliable myoelectric control provided by the surface electrodes. We addressed these problems with a combination of surgical reconstruction procedures together with an electromechanical interface for prosthesis attachment and bidirectional communication with implanted electrodes. This neuromusculoskeletal interface was implanted in three different stages. First, a titanium fixture was implanted intramedullarily and left undisturbed to enable osseointegration (fig. S1). Six months later, a percutaneous component (abutment; fig. S1) was coupled into the fixture, allowing for the skeletal attachment of the prosthetic arm and thus addressing the patient's socket-related discomfort. The limited and unreliable prosthetic control was then addressed in a third surgery by reconstructing the neuromuscular structures within the residual limb and instrumenting them with implanted electrodes (fig. S1).

The median nerve was dissected longitudinally into four groups of fascicles to reinnervate the brachialis muscle and three free muscle grafts (fig. S1). Similarly, the ulnar nerve was divided into two parts to innervate the short head of the biceps muscle and one free muscle graft (fig. S1). The radial nerve was divided into two parts to then reinnervate the lateral head of the triceps muscle and one free muscle graft (fig. S1). The neuromas located at the end of these nerves were transected before dissection and transfer. The nonvascularized muscle grafts were obtained from the vastus lateralis muscle in the thigh.

Intramuscular electrodes were inserted into native muscles and into the free muscle grafts. Epimysial electrodes were implanted on each head of the biceps muscle as well as on the lateral and long heads of the triceps muscle (fig. S1). A cuff electrode with a mixed tripolar contact configuration (*11*) was implanted around one of the fascicles of the median nerve (fig. S1). Communication between the implanted electrodes and the outside of the body was achieved through the osseointegrated implant within which feedthrough mechanisms allowed for bidirectional signal transmission while sealing the interface (*9*). A revision surgery for the skin interface was performed to remove excess granulation tissue at week 65 after implantation of electrodes. The patient was treated with antibiotics after superficial skin infections at weeks 94, 135, and 171 and after a deep soft-tissue infection at week 116 after implantation of electrodes.

Neuromusculoskeletal interface stability

The stability of the neuromusculoskeletal interface was examined by monitoring the electrical resistance of each implanted electrode over time. The resistance of the epimysial electrodes ranged

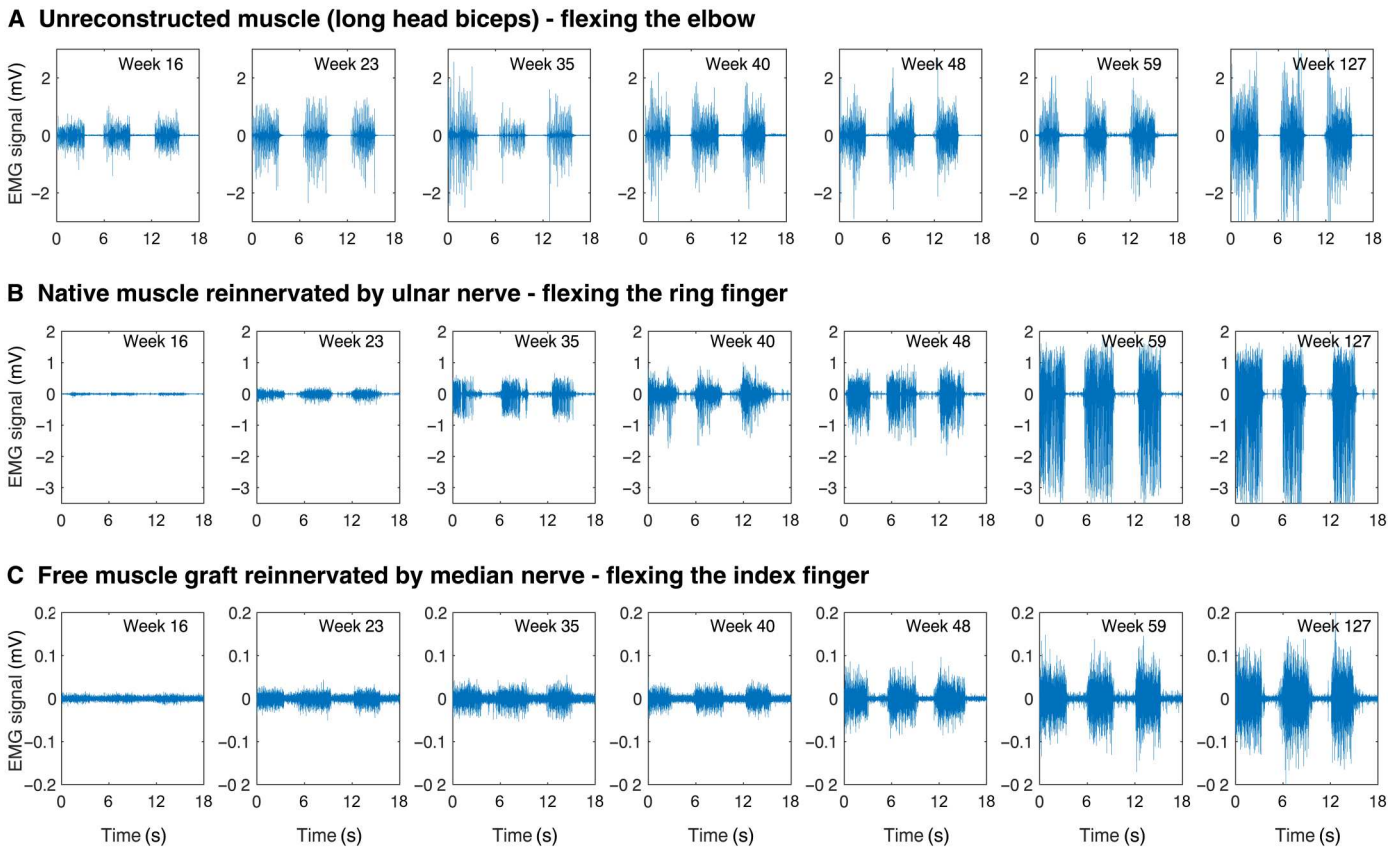

Fig. 2. Representative examples of raw EMG signals over time. Shown are representative raw EMG signals for electrodes in an unreconstructed muscle (long head of the biceps brachii) of the patient (**A**), a native muscle reinnervated by the ulnar nerve (**B**), and a free muscle graft reinnervated by the median nerve (**C**). Each EMG recording consists of 3-s sequences of three active movements and three rest periods.

between 1.3 and 1.9 kilohms at 4 weeks after implantation and stabilized at 1.4 and 1.6 kilohms (Fig. 1A) 2 years after implantation. Similarly, the resistance of the intramuscular electrodes ranged between 250 and 1400 kilohms at 4 weeks after implantation and then 740 and 1300 kilohms (Fig. 1B) 2 years after implantation. The cuff electrode has two types of contacts (*11*): ring and discrete. The resistance of the ring contact was 1.5 kilohms at 4 weeks after implantation and 1.5 kilohms 2 years after implantation, and the resistance of the three discrete contacts ranged between 15 and 20 kilohms at 4 weeks after implantation and 5.1 and 14 kilohms after 2 years (Fig. 1C). The resistance values for the intramuscular electrodes did not show a statistically significant change over time ($P = 0.41$). The resistance values of the epimysial and cuff electrodes decreased slightly during the second year ($P = 0.041$ and 0.026, respectively). One intramuscular electrode was considered an outlier and excluded from the aforementioned range and further analyses, because it increased from 1.3 to 141 kilohms between 40 and 127 weeks after implantation. This abnormally large increment was most likely due to damage to the external connector pin. For an overview of all resistance values, see table S1.

Reinnervation development and myoelectric signal quality

The development of the signal quality of the different implanted electrodes was quantified by calculating the signal-to-noise ratio (SNR). As expected, weeks were required for the functional reinnervation of all muscular constructs, as opposed to the unreconstructed muscles from which electromyographic (EMG) activity was readily available directly after implantation. Relevant signs of reinnervation were observed 23 weeks after implantation (examples in Fig. 2). Exceptions were the muscles reinnervated by the radial and median nerves, which began to display information about single finger actuation at around 40 weeks after implantation.

Soon after the surgery, the four electrodes placed in unreconstructed muscles displayed an average SNR of 23.3 ± 6.1 dB (Fig. 3A) and remained nearly constant over time, with an average SNR of 24.1 ± 5.4 dB at the end of the experimental period. The average SNR of the three electrodes in the reinnervated native muscles started at 1.6 ± 5.4 dB and increased to 19.4 ± 6.4 dB (Fig. 3B). All three electrodes in reinnervated muscles showed a significant increase in SNR over the 127 weeks of the experimental period ($P = 5.8 \times 10^{-9}$, 3.8×10^{-6}, and 1.3×10^{-4} for the radial, ulnar, and median electrodes, respectively). The electrodes in the five free muscle grafts started with an average SNR of 1 ± 0.8 dB and developed up to an average SNR of 17.8 ± 2.4 dB (Fig. 3C). A significant SNR increase was observed over the 2-year period since electrode implantation for the radial ($P = 2.7 \times 10^{-11}$), ulnar ($P = 8.4 \times 10^{-10}$), and the three median electrodes ($P = 2.4 \times 10^{-14}$, 9.3×10^{-5}, and 1.5×10^{-7}, respectively). For an overview of all SNR values, see table S2.

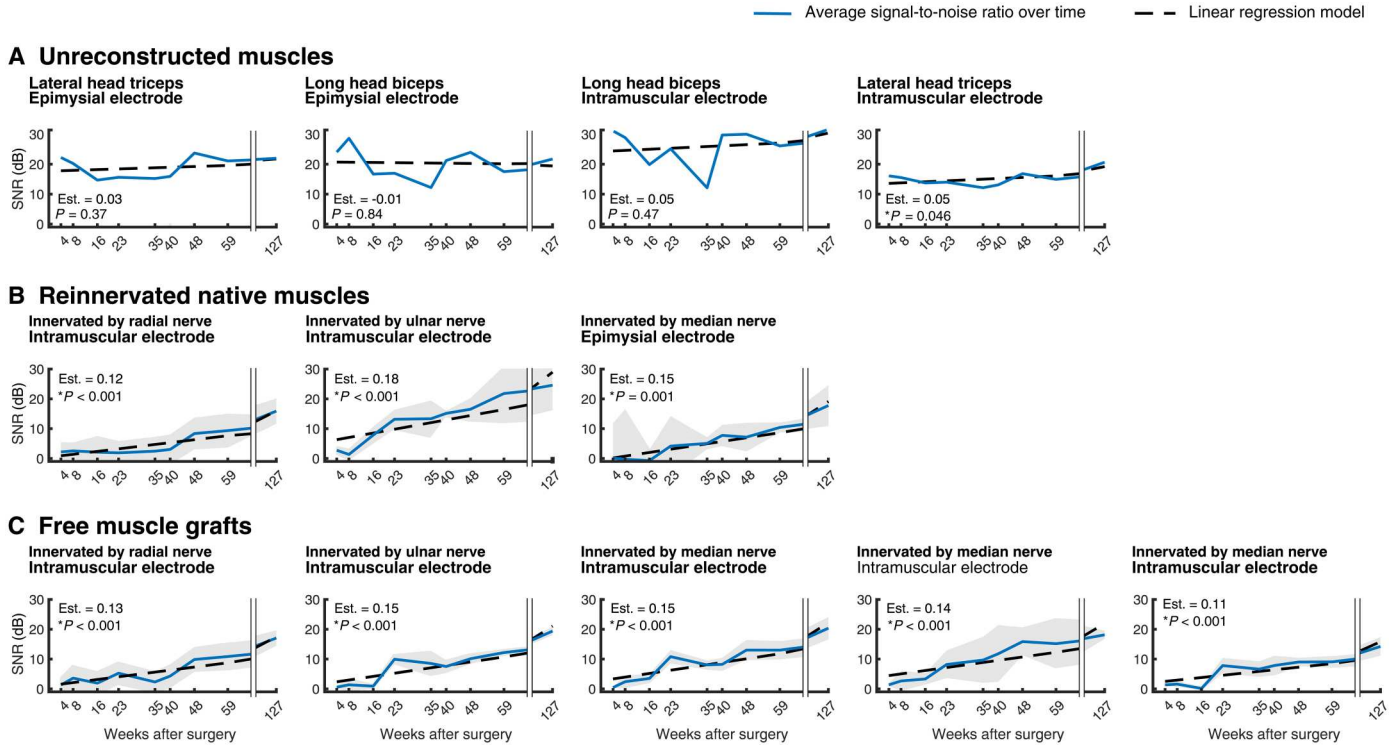

Fig. 3. SNR changes over time. Shown are changes in signal-to-noise ratio (SNR) of (**A**) four electrodes in unreconstructed muscles ($n = 1$ movement), (**B**) three electrodes on/in reinnervated native muscles ($n = 6$, 3, and 4 movements from left to right, respectively), and (**C**) five electrodes within reinnervated free muscle grafts ($n = 6$, 3, 5, 3, and 3 movements from left to right, respectively). The gray areas depict the SD around the average values over the number of movements. For all SNR calculations, only data of the main movements that anatomically corresponded to the electrode placement/innervation site were considered.

Decoding of motor volition

We decoded the intended movements of the missing arm and hand in two groups: nine gross movements and 11 finger movements. Gross movements consisted of hand opening/closing, wrist pro/supination, wrist flexion/extension, elbow flexion/extension, and no movement (rest). Finger movements consisted of all five fingers flexion/extension and no movement. We used information from all electrodes to compute offline and real-time classification performance by linear discriminant analysis. The motion test (*2*) as implemented in the open-source platform BioPatRec (*12*) was used to evaluate offline and real-time decoding in a laboratory environment.

Gross movements

The offline accuracy steadily increased within the first 23 weeks after implantation and remained between 95.8 and 99.3% (Fig. 4A). The patient successfully completed the motion test with gross movements at 16 weeks after implantation (Fig. 4B). Over the duration of the experiment, the completion time for a single gross movement decreased from 4.0 ± 0.1 to 1.8 ± 0.7 s, with the minimum completion time being 1.2 ± 0.2 s (Fig. 4C). Correspondingly, the online accuracy of classifying all eight gross movements increased significantly from 36 ± 4 to 66 ± 16% ($P = 0.005$), with a maximum of 75% 48 weeks after implantation (Fig. 4D). For an overview of the motion test metrics for gross movements, see table S3.

Single finger movements

The offline accuracy increased within the first 16 weeks and then remained between 86.7 and 96.8% over the next 2 years (Fig. 4E). The average completion rate of the motion test for single finger decoding increased from 13 ± 35 to 100% between the first and the last training sessions (Fig. 4F). The average time for completion significantly decreased ($P = 0.05$) from 7.0 ± 0.6 s down to 1.6 ± 0.6 s (Fig. 4G). The average online classification accuracy increased significantly ($P = 1.9 \times 10^{-5}$) from 6 ± 3 to 69 ± 6% (Fig. 4H). For an overview of the motion test metrics for finger movements, see table S4.

Functional outcomes

We measured prosthetic function using the Assessment of Capacity for Myoelectric Control (ACMC) *(13)* and found that the ACMC composite score improved by 16.7% at 59 weeks after the intervention (from 32.2 to 37.6; Fig. 5A) using intuitive control with signals from the newly created myoelectric sites. No improvement was observed at 8 weeks after the intervention (32.2 to 30.3; Fig. 5A) using nonintuitive control with signals from unreconstructed native muscles. The ACMC test was performed using a conventional prosthesis with socket attachment and surface electrodes before the intervention as well as skeletal attachment and implanted electrodes after the intervention. The prosthesis consisted of a single-DoF myoelectric hand (MyoHand VariPlus Speed, Ottobock) and an elbow (ErgoArm, Ottobock) with a myoelectric locking system (1.5 DoFs combined). When taking advantage of all the myoelectric sites by using a 4.5-DoF control scheme (allowing for simultaneous and proportional control of the thumb, index finger, middle/ring/little fingers, wrist rotation, and elbow lock/unlock), the patient

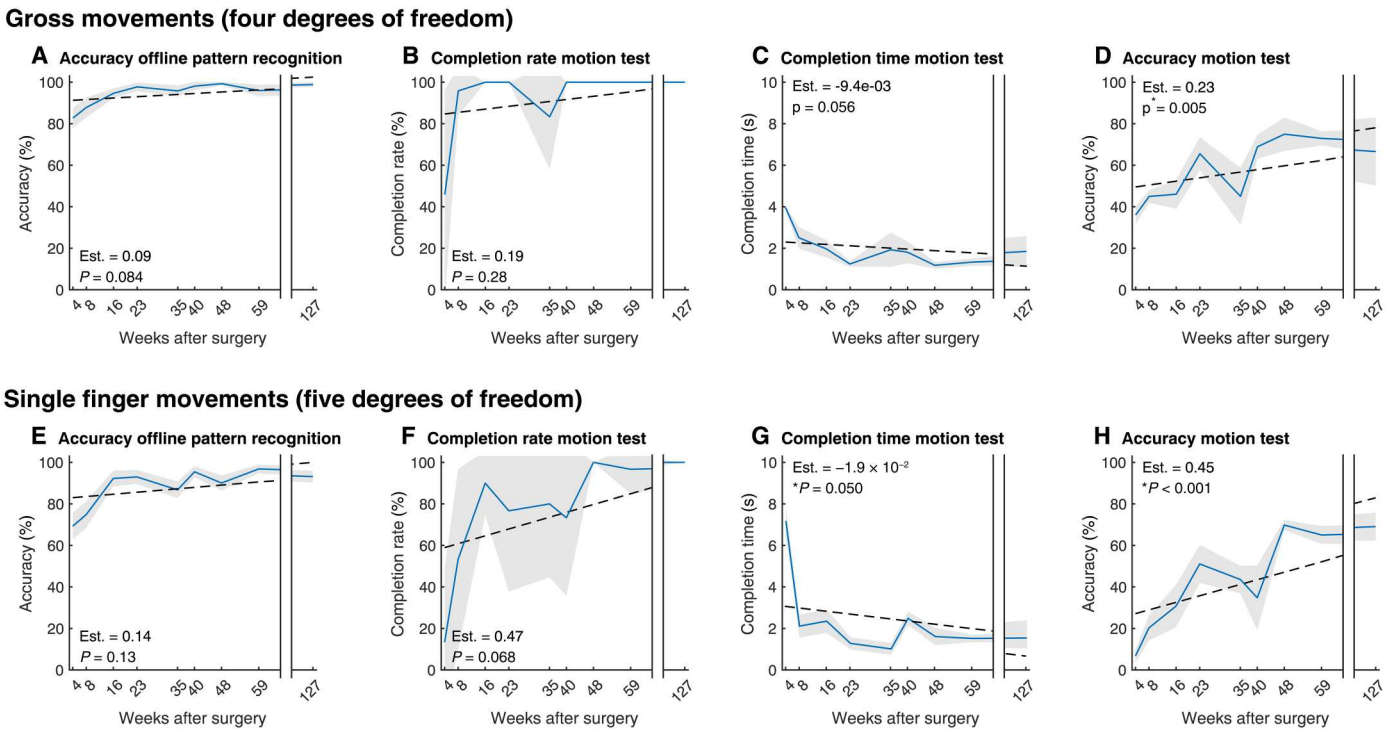

Fig. 4. Offline and online decoding performance. Shown is decoding performance in the single patient using gross movements (hand opening/closing, supination/pronation, wrist flexion/extension, and elbow flexion/extension) and single finger movements over a 2-year period after surgical intervention. (**A**) Offline accuracy of nine gross movements (n = 9 movements, 100 repetitions) is shown. (**B**) Motion test completion rate for gross movements (n = 9 movements, three trials), where 100% indicates that all required movements were performed, is shown. (**C**) Completion time (time between the first decoded movement and 20 correct predictions of the promoted movement) and (**D**) accuracy (percentage of correct predictions) for the 4 DoFs during the motion test are shown. (**E**) Offline accuracy of individual fingers (n = 11 movements, 100 repetitions) is shown. (**F**) Completion rate, (**G**) completion time, and (**H**) accuracy for the motion test for individual finger decoding (n = 11 movements, three trials each) are shown.

achieved the highest improvement at 39.8% (ACMC score: 45.0; Fig. 5B). This was despite using such a system for the first time (untrained). The 4.5-DoF prosthesis consisted of a multiarticulated myoelectric hand (BeBionic, Ottobock), a wrist rotator (Ottobock), and an elbow (ErgoArm, Ottobock) with a myoelectric locking system. Conversely, the Southampton Hand Assessment Procedure (SHAP) score improved both at 8 and 59 weeks after intervention by 42.6 and 82.7%, respectively (24.9 to 35.5 and 45.8; Fig. 5C). Using the 4.5-DoF control scheme with the electro-neuromuscular constructs, the SHAP score doubled to 50.1 (101.2%) compared with conventional surface electrodes (Fig. 5D). For an overview of the functional outcome values, see table S5.

DISCUSSION

In this study, we present a combination of surgical reconstruction procedures together with a long-term stable neuromusculoskeletal interface. Thanks to the wired access to the implanted electrodes provided by the neuromusculoskeletal interface, it was possible to track signal development over a period of 2 years. The signal development was analyzed in terms of stability (electrical resistance), quality (SNR), and feasibility for advanced prosthetic control based on myoelectric pattern recognition (offline and in real-time decoding). Aside from confirming the long-term stability of the interface and strengthening of the myoelectric signals over time, we have shown that nerve transfer to denervated native muscles and nonvascularized free grafted muscles increased the number of myoelectric sources for prosthetic control to ultimately allow for independent control of all five fingers (demonstration in movie S1).

The final number of reinnervation sites depended on the number of fascicles that could be dissected without compromising naturally occurring fascicle crossings within the nerve trunk. Larger diameter nerves, such as the median nerve, allowed for more dissectible fascicles (four in our study) than smaller ones, such as the radial nerve (two fascicles in our study). The number of dissectible fascicles can vary from person to person and the level of amputation. Electrode selection, on the other hand, depends on the type of muscular target. The free muscle grafts are nonvascularized and are therefore dependent on blood diffusion from surrounding tissue for survival, although vessels within the innervating fascicle can also contribute. Placing an epimysial electrode would compromise blood diffusion in a relatively large surface area, and therefore intramuscular electrodes are preferred for this muscular target. Native muscles are vascularized, and both epimysial and intramuscular electrodes have been used successfully in this case.

We used the electrical resistance to each electrode as a metric of long-term stability of the interface, because extreme high or low values would indicate an interruption of continuity (open circuit) or a loss of independent connection (short circuit), respectively. Both scenarios would compromise the use of the implanted

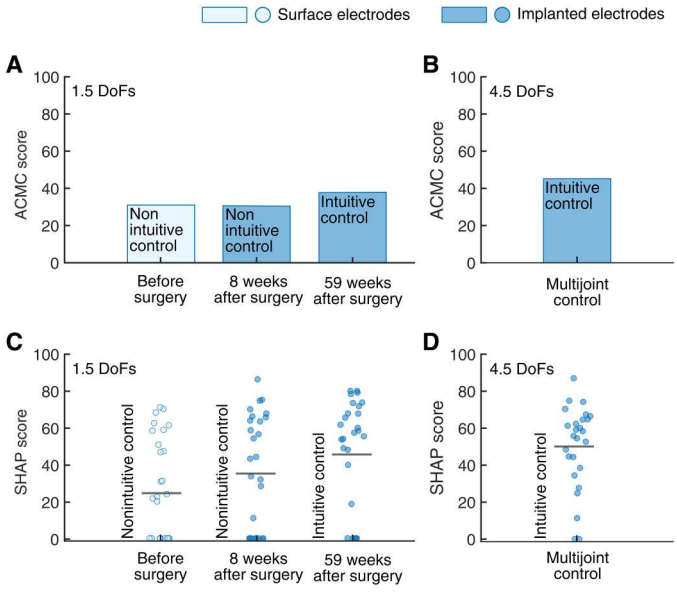

Fig. 5. Performance on functional tests. (**A**) Shown are outcomes for the ACMC test, scored between 0 and 100, for a 1.5-DoF control scheme using surface electrodes before surgery and implanted electrodes at weeks 8 and 59 after surgery. A higher score indicates a higher capacity for myoelectric control of the prosthesis. (**B**) Shown are ACMC test outcomes when using a 4.5-DoF simultaneous and proportional control scheme with the electro-neuromuscular constructs and without previous training. (**C**) Shown are outcomes on the SHAP test for the patient with surface electrodes before surgery and implanted electrodes at weeks 8 and 59 after surgery. The circles indicate the linear index of function, scored between 0 and 100, for each task of the SHAP test (n = 26 tasks). The horizontal black lines show the weighted linear index of function, where a higher score represents greater prosthetic functionality during activities of daily living. (**D**) Shown are outcomes on the SHAP test (n = 26 tasks) when using a 4.5-DoF simultaneous and proportional control scheme with the electro-neuromuscular constructs and without previous training.

electrodes and interface for prosthetic control. We found that the electrical resistance of the implanted electrodes (including leads and feedthrough connectors) remained stable within functional bounds. These results are in accordance with the long-term electrical stability of previously reported individuals who received neuromusculoskeletal interfaces (*7*, *9*).

We found that the transected nerves effectively innervated the native muscles and free muscle grafts at about 5 (ulnar and median nerves) and 11 months (radial nerve) after surgery. The innervation process led to distinct myoelectric signals appearing on the different electrodes and a notable increase in SNR. As expected, the epimysial electrodes placed on unreconstructed native muscles, not having to reinnervate, featured myoelectric signal activity soon after the surgery and exhibited a stable and slightly increasing SNR over the 127 weeks of the study.

Previously, in two patients with transhumeral amputation (*14*), we tracked the reinnervation of the radial and ulnar nerves into denervated native muscles, reaching an average SNR of 20 and 26 dB, respectively. Here, we report an average of 19.4 dB for similarly reinnervated native muscles, despite using monopolar electrodes as opposed to the bipolar electrodes used in our previous study. When restricted by the number of possible electrode contacts in an implant system, using monopolar electrodes allows for instrumenting more targets with the downside of reducing SNR compared with a bipolar electrode configuration. Our results indicate that this is an acceptable trade-off when considering that more information can be obtained by adopting a monopolar electrode strategy.

In a study by Vu *et al.* (*6*), seven patients with upper limb amputation underwent regenerative peripheral nerve interface surgery for the treatment of neuroma pain. Three of the patients were implanted with intramuscular electrodes with percutaneous leads 1 to 3 years after surgery. They reported an average SNR of 4.2 dB with fine wire electrodes, 68.9 dB (after a 3-year reinnervation period), and 21.0 dB (after a 1-year reinnervation period) with intramuscular bipolar electrodes. These SNR values are comparable to our findings for similarly reinnervated free muscle grafts at 2 years after surgery despite using monopolar electrodes (maximum: 21.7 dB and average: 17.8 dB) and therefore expecting lower SNR values compared with a bipolar configuration. The two patients with intramuscular electrodes in native and reconstructed muscles in Vu *et al.*'s study (*6*) were able to control some finger movements (thumb, ring finger, and small finger flexion; thumb opposition; as well as concurrent abduction and adduction of all fingers), albeit limited to four movements at a time. These patients had transradial amputations, and therefore some of the native muscles responsible for finger control were available, as opposed to a transhumeral amputation where all muscles related to finger control are lost. For a person with a transhumeral amputation who underwent targeted muscle reinnervation, Osborn *et al.* (*15*) demonstrated, in a video recording, the real-time individual flexion of up to three fingers at the time, with combined extension, effectively decoding four movements. In comparison with these studies, we believe that the considerable increase in prosthetic control reported here (independent flexion and extension of all five fingers) was made possible by combining different surgical techniques and thereby creating notably more sources for myoelectric control.

Over the duration of our investigation, the patient's ability to differentiate hand movements improved steadily. Our patient successfully completed motion tests with gross movements (4 DoFs) at 16 weeks after implantation, with faster completion times and increasing accuracy over time. Concurrently with the innervation of the radial nerve, the patient completed the motion test with single finger movements (5 DoFs) at 48 weeks after implantation. Similar completion times and accuracies were achieved in both sets of movements (gross and single finger). Kuiken *et al.* (*2*) performed targeted muscle reinnervation surgery on five participants (three with shoulder disarticulation and two with transhumeral amputation) and investigated real-time decoding of 10 elbow, wrist, and hand movements using surface electrodes. They reported an average offline classification accuracy of 95% and motion test completion rates of 86.9 and 96.3% with completion times of 1.54 and 1.29 s for four hand movements and for six elbow and wrist movements, respectively. Another study by Cipriani *et al.* (*16*) also demonstrated the feasibility of real-time finger control, albeit in transradial amputees as opposed to a transhumeral amputee. They reported the decoding of seven movements, four of which were flexing individual fingers, with an average motion test completion rate of 79 ± 16%. In comparison with these studies, we assume that our patient was able to achieve higher completion rates (100%)

because of the combination of surgical reconstruction and permanently implanted electrodes.

Reliability in daily use has been reported as the main factor for prosthesis acceptance (*17*). Our reported motion test accuracy (69 to 75%) might suggest low reliability, despite being higher than that previously reported, to yield acceptable prosthesis control (*18*). Decoding accuracy is not synonymous with controllability. Spurious misclassifications are common in decoders but do not translate necessarily to noticeable errors during prosthetic control, because classification output is continuously overwritten and low pass–filtered by the motors in the prosthesis. For the motion test experiment, the patient was asked to perform preselected movements intuitively during the recording session, without previous training of the movements. Exploring the signal space together with the patient to find and train more distinguishable, yet still intuitive, signal patterns for the different movements would likely lead to an improvement in decoding consistency.

The predefined movements for the motion test experiment were selected to showcase the potential of the surgical reconstruction approach. To increase reliability during home use, a subset of all the movements can be chosen instead. For example, only actuating the thumb and index finger individually and actuating the middle, ring, and little fingers as one movement decrease the complexity of control while still offering considerable functional improvements. A sequential decoding scheme, meaning that only one movement is output at a time, limits functionality during home use. Simultaneous control would increase the functional benefits during home use, especially for finger movements (closing individual fingers sequentially to perform a grasp would be slow, unintuitive, and frustrating). Adding proportionality could further contribute to reliability and intuitiveness.

On the basis of the above-described considerations, we used a 4.5-DoF (thumb, index finger, middle/ring/little fingers, wrist rotation, and elbow lock/unlock) simultaneous and proportional control scheme to evaluate the functional benefits of a higher DoF controller made possible by the additional myoelectric sources created by the surgical reconstruction. The use of the neuro-musculoskeletal prosthesis resulted in an increase of 12.8 points on the ACMC test; however, the minimum detectable change was 14.5 points (*19*), from 32.2 to 45.0; there was also a doubling of the SHAP score from 24.9 to 50.1 compared with the standard two-site surface EMG electrode prosthesis used before the surgical intervention. Even when using the same control scheme (1.5-DoF direct control), the intuitive control and the added reliability from having the electrodes implanted led to an increase in prosthetic functionality (ACMC score increased from 32.2 to 37.6, and the SHAP score increased from 24.9 to 45.8) compared with the two-site surface electrode prosthesis used before the intervention. These results indicate that electro-neuromuscular constructs using implanted electrodes can lead to greater capacity for myoelectric control and thereby functionality for everyday tasks (demonstration in movie S2).

The improvements in functionality were achieved despite the patient only having used such a prosthesis for a couple of hours. We therefore assume that the intuitive control granted by the newly created myoelectric sources greatly facilitated learning a more complex control scheme. Given the improvement in functionality that we observed when the patient used the 1.5-DoF prosthesis over an extended time at home, we predict that prolonged use of the 4.5-DoF prosthesis could lead to further functional improvements to facilitate activities of daily life.

There are several limitations to our study. The main limitation is that only one patient was treated with this new surgical approach. In addition, we did not compare the surgical nerve transfer to native muscles versus free muscle grafts but rather aimed to evaluate the feasibility of doing this concurrently. Although the nerve transfers would not have been successful, the patient would have still enjoyed improved prosthetic control and sensory feedback using unreconstructed sites (*7*, *20*), which was an important ethical consideration. Because of constraints on the patient′s availability, we performed only one set of functional tests during each follow-up. Therefore, another limitation of our study was that we did not disentangle the separate contributions to improvement of (i) electrode type (surface versus implanted), (ii) intuitiveness of control (native residual muscles versus surgically reconstructed myoelectric sites), and (iii) potential learning effects (*21*). The SHAP score but not the ACMC score showed improvement early after intervention when the control scheme was nonintuitive, and both scores showed improvement later at week 59, when the control was intuitive using the new surgically reconstructed myoelectric sites and the patient was more experienced. Further systematic work is needed to disentangle the contribution of each variable.

We observed undesired cross-talk between myoelectric sites that can be attributed to several causes, such as the placement of the electrodes, the location of the electro-neuromuscular constructs, the use of monopolar electrodes, and the nature of the neuromuscular constructs themselves, because they often share neural information related to the same movements. Greater attention to the placement of electrodes and neuromuscular constructs can reduce signal cross-talk, but not entirely. Intraoperative identification of nerve fascicles during reconstruction remains challenging, but achieving this would considerably improve the creation of optimal neuromuscular control sources. On the engineering side, recent advances in source separation algorithms are a promising approach for decoding movement intent, offering insights into the discharge patterns of motor neurons (*22*, *23*). It has been shown that neural and myoelectric information can be combined to achieve more independent control of different prosthetic joints (*24*, *25*).

In this proof-of-concept study, we have demonstrated the feasibility of transferring severed nerves to native muscles and free muscle grafts, resulting in long-term stable electro-neuromuscular constructs using implanted electrodes that can be safely and reliably accessed using a neuromusculoskeletal interface. Safety and reliability are prerequisites for the clinical implementation of new prosthetic technologies. By merging surgical and engineering technologies, our approach allows for a more comfortable use of the prosthesis (*26*), a more functional load transfer between the prosthesis and the skeleton (*27*, *28*), and a more reliable and precise control of the prosthesis (*8*, *9*). Our approach opens up possibilities for a more advanced and dexterous control of a prosthetic hand supported by tactile sensory feedback (*9*, *29*) and contributes to the wider clinical application of osseointegration and advanced surgical reconstruction to improve artificial limb replacement.

MATERIALS AND METHODS

Study design

In this study, we investigated whether creating electro-neuromuscular constructs using distributed nerve transfers to different types of muscle targets instrumented with implanted electrodes could increase the number of myoelectric sources for control of a prosthesis. The main prespecified study objective was to assess whether additional myoelectric sources could be created by transferring nerves to native and free grafted muscles, which could then be used to decode motor volition (as measured by the motion test). The secondary prespecified objective was to assess the innervation and development of the different surgical constructs over time measured by the SNR. In addition, we evaluated prosthetic function during tasks representative of daily life (measured by the ACMC and SHAP tests).

A 51-year-old male patient with a transhumeral amputation because of a traumatic injury in July 2015 participated in this study. The first surgical stage, implanting the titanium fixture, was performed in September 2017. The percutaneous component of the implant system was coupled into the fixture in February 2018. The third surgical stage (the basis for the current study), which involved reconstructing the neuromuscular structures within the stump and instrumenting them with electrodes, was performed in December 2018.

Data were collected over a period of 1 year at eight periodic follow-up appointments (7.8 ± 2.9 weeks between visits) and at a follow-up visit 2 years (127 weeks) after reconstruction and electrode implantation. Functional outcome data were collected before surgery and at 8 and 59 weeks after the last surgery. An additional round of functional tests with a multi-DoF prosthesis was conducted 215 weeks after the last surgery. During the time of this 2-year study, the patient first used a prosthesis, allowing for a DoF of 1.5 (hand opening/closing and elbow lock/unlock) for daily home use. At week 65, the patient was fitted with an additional DoF prosthesis (pronation/supination) (*21*). At 181 weeks after the surgery, the patient was also provided with an active elbow, allowing him to control a total of 3 DoFs for daily home use. In all cases, a direct control approach was used, allowing for simultaneous and proportional control of the individual DoF.

The study protocols were carried out in accordance with the declaration of Helsinki. Signed informed consent was obtained before conducting the experiments. The study was approved by the Regional Ethical Review Board in Gothenburg, Sweden (Dnr. 18-T125).

Surgical reconstruction and implantation

The radial nerve was exposed through a curvilinear incision proximally in the arm at its exit from the triangular interval. Branches to the lateral, long, and medial heads of the triceps were identified with the help of a nerve stimulator and isolated. The motor branch to the lateral head of the triceps was left intact, whereas the main branch to the long head was severed 5 mm before its entrance into the muscle and marked for later neurotization. The main trunk of the radial nerve was then followed distalward, and its stump retracted proximally. Once the large end neuroma was excised, the healthy-looking fascicles were split longitudinally into two halves. One half was anastomosed to the motor branch, supplying the long head of the triceps. The other half lay in the center of a nonvascularized muscle graft, which was folded around the nerve following the principle of a regenerative peripheral nerve interface (*4*, *5*).

An anterior curvilinear incision in the arm gave access to the two major nerves, median and ulnar, as well as the musculocutaneous nerve that was identified in the groove between the long and short heads of the biceps muscle. The long head maintained its original innervation, whereas the motor branch of the short head was severed 5 mm before its entrance into the muscle. The distal stump of the ulnar nerve was identified and retracted proximally, and its neuroma was excised. Similar to the radial nerve, the ulnar nerve was split longitudinally into two halves: One was sutured to the motor branch of the short head of the biceps, and the remaining half was placed in a nonvascularized muscle graft. The distal stump of the median nerve was identified and retracted proximally, and the large neuroma stump was excised. The nerve was divided longitudinally into four groups of fascicles: One was reserved for sensory feedback and wrapped with an extraneural electrode; the remaining three were used to reinnervate nonvascularized muscle grafts. All of the free muscle grafts were harvested from the vastus lateralis muscle in the homolateral thigh and had a standard dimension of 5 by 3 by 1.5 cm.

Neuromusculoskeletal interface stability

The stability of the neuromusculoskeletal interface was examined over time by monitoring the electrical resistance of each implanted electrode. The resistance was computed by applying Ohm's law to the voltage caused by a single current-controlled electrical pulse with known parameters (current amplitude: 100 or 200 μA and pulse width: 100 μs). The voltage was measured via an oscilloscope and an isolated differential probe.

Myoelectric signals acquisition

During each follow-up, two EMG recording sessions were performed from all implanted muscular electrodes. The recording sessions were performed using BioPatRec (*12*), an open-source platform for research on myoelectric pattern recognition, and the Artificial Limb Controller, an embedded system for controlling prosthetic devices (*30*). EMG monopolar data were sampled at 500 Hz with a 16-bit resolution and online high-pass– and notch-filtered at 20 and 50 Hz, respectively.

For each recording session, the patient was asked to comfortably sit in front of a computer and follow on-screen instructions to perform a preselected set of movements. This study focused on two different sets of movements, defined as "gross" and "single finger" movements. The gross movements set included open and close hand, supination and pronation, flex and extend wrist, as well as flex and extend elbow. The single finger movements set included flexion and extension of all digits, i.e., thumb, index, middle, ring, and pinky fingers. For every set, each movement was repeated three times, alternating 3 s of muscular effort and 3 s of resting time. The patient was asked to perform each movement at approximately 70% of maximum voluntary contraction.

Myoelectric signal quality

The development of the signal quality of the different implanted electrodes was quantified by calculating the SNR. For each recorded channel, the recording session was divided into segments containing the voluntary contraction information of each movement and segments containing the resting state signal. Solely, the steady

state of the EMG signal was considered; thus, the SNR was calculated on the middle 70% samples of each segment [see Mastinu *et al.* (*14*) for a similar approach]. Furthermore, only the movement data that anatomically corresponded to the electrode placement were considered to calculate the SNR of each of the individual electrodes. For calculating the SNR of the two electrodes on/in the unreconstructed lateral head triceps and for the two electrodes on/in the unreconstructed long head biceps, only the recorded elbow extension movement and only the recorded elbow flexion movement were used. For the electrodes placed on/in sites innervated by fascicles of the radial nerve, recordings of pronation, extend elbow, and extension of all fingers were used if activation was present. Hand, ring finger, and pinky flexion movements were used to calculate the SNR values of the electrodes on/in sites innervated by fascicles of the ulnar nerve. For the electrodes in sites innervated by fascicles of the median nerve, supination; hand flexion; as well as thumb, index finger, and middle finger flexion were considered if activation was present. Last, the root mean square values were calculated, and then the SNR was obtained according to the Eq. 1

$$\mathrm{SNR_{dB}} = 10^{*}\log_{10}\frac{\mathrm{EMG^2_{RMS,Movement(s)}}}{\mathrm{EMG^2_{RMS,Rest}}} \quad (1)$$

We considered native muscles and free muscle grafts to be effectively innervated at a sustained SNR of four and higher.

Myoelectric pattern recognition

Offline pattern recognition accuracy

The EMG data from the recording sessions were segmented into overlapping time windows of 200 ms (time increment: 50 ms). The Hudgins′ set of features (*31*) (mean absolute value, zero crossing, waveform length, and slope changes) was extracted from each time segment. The obtained features were randomly divided into training, validation, and test sets with a ratio of 40, 20, and 40%, respectively. Then, these sets were fed to a linear discriminant analysis classifier for supervised training. Last, the training was repeated 100 times, and the resulting averages, for both sets of movements, were reported.

Real-time pattern recognition accuracy

The real-time classification accuracy was assessed via the motion test introduced by Kuiken *et al.* (*2*) as implemented in BioPatRec (*12*). In this test, the patient was asked to perform movements randomly prompted on a screen. For every requested movement, 20 noncontiguous classifications had to be correct within 10 s to deem the particular movement completed. From this, several metrics were calculated: completion rate as the percentage of completed motions, completion time as the time between the first correct prediction and the completion of the motion, and real-time accuracy as the percentage of correct predictions over the total number of predictions during the completion time. The motion test was repeated three times for each set of movements, gross and single finger movements. The average results and SD over the three trials are reported.

Functional outcomes

Prosthetic functionality was evaluated before and after the surgical intervention using the ACMC test (*13*) and the SHAP test (*32*). The ACMC test measures a person′s ability to perform daily tasks, scoring 22 aspects of prosthetic use on a four-point rating scale with a maximum of 66 points per task. A normed composite score between 0 and 100 can be obtained from the raw score via Rasch analysis, where a composite score above 57.2 is classified as "extremely capable." The SHAP test consists of two parts: The first part involves 12 tasks where the patient grasps and relocates abstract-shaped objects; and the second part involves 14 tasks of activities of daily living, such as turning a door handle, unbuttoning a shirt, and opening a jar. The execution times of all 26 tasks were used to calculate the weighted linear index of function, a normed score where a score of 100 indicates normal hand function (*33*).

The patient′s habitual two-site surface EMG electrode prosthesis (one electrode pair placed on the biceps and triceps muscles, respectively) with a direct control scheme was used for the preoperative tests, and the neuromusculoskeletal interface was used for postoperative tests. A 1.5-DoF direct control scheme based on electrodes in the native biceps and triceps muscles (i.e., nonintuitive control) was used to control the prosthesis for the tests at 8 weeks after surgery. At 59 weeks after surgery, a 1.5-DoF direct control scheme based on signals from the surgically created myoelectric sites was used to allow for intuitive opening (mapped to the signal from a free muscle graft reinnervated by median nerve) and closing (mapped to the signal from a native muscle reinnervated by ulnar nerve) of the prosthetic hand and lock/unlocking of the elbow (mapped to the signal from the native biceps). In both cases, the patient used the same control during daily life before the tests.

To demonstrate the functional benefits of the higher DoF controllers, the patient also performed the tests using a 4.5-DoF simultaneous and proportional controller. The 4.5-DoF controller allowed individual control of the thumb, index finger, middle/ring/little fingers, wrist rotation, and elbow lock/unlock. For example, simultaneous activation of the thumb and index finger allowed the patient to pinch, and simultaneous movement of all fingers allowed for hand opening and closing. The control scheme was composed of a multilayer feed-forward neural network capable of multilabel classification (*18*) and a post hoc proportionality algorithm taking the predicted class and the current mean absolute value into account. Prosthetic function with the 4.5-DoF controller was tested without previous training.

Statistical analysis

To evaluate the development of electrode impedance, the signal quality, and the offline and real-time pattern recognition accuracies over time, we performed a linear regression analysis as implemented in the "fitlm" function of MATLAB′s Statistics Toolbox (MathWorks, USA). For each linear regression analysis, we report the estimate (the slope of the linear regression) and the *P* value (outcome of the *t* statistic with the hypothesis test that the estimate is different to zero).

Supplementary Materials

This PDF file includes:

Fig. S1

Tables S1 to S5

Other Supplementary Material for this manuscript includes the following:

Movies S1 and S2

MDAR Reproducibility Checklist

View/request a protocol for this paper from *Bio-protocol*.

REFERENCES AND NOTES

1. M. Ortiz-Catalan, Engineering and surgical advancements enable more cognitively integrated bionic arms. *Sci. Robot.* **6**, eabk3123 (2021).
2. T. A. Kuiken, G. Li, B. A. Lock, R. D. Lipschutz, L. A. Miller, K. A. Stubblefield, K. B. Englehart, Targeted muscle reinnervation for real-time myoelectric control of multifunction artificial arms. *JAMA* **301**, 619–628 (2009).
3. L. A. Miller, R. D. Lipschutz, K. A. Stubblefield, B. A. Lock, H. Huang, T. W. Williams, R. F. Weir, T. A. Kuiken, Control of a six degree of freedom prosthetic arm after targeted muscle reinnervation surgery. *Arch. Phys. Med. Rehabil.* **89**, 2057–2065 (2008).
4. M. G. Urbanchek, Z. Baghmanli, J. D. Moon, K. B. Sugg, N. B. Langhals, P. S. Cederna, Quantification of regenerative peripheral nerve interface signal transmission. *Plast. Reconstr. Surg.* **130**, 55–56 (2012).
5. M. G. Urbanchek, T. A. Kung, C. M. Frost, D. C. Martin, L. M. Larkin, A. Wollstein, P. S. Cederna, Development of a regenerative peripheral nerve interface for control of a neuroprosthetic limb. *Biomed. Res. Int.* **2016**, 1–8 (2016).
6. P. P. Vu, A. K. Vaskov, Z. T. Irwin, P. T. Henning, D. R. Lueders, A. T. Laidlaw, A. J. Davis, C. S. Nu, D. H. Gates, R. B. Gillespie, S. W. P. Kemp, T. A. Kung, C. A. Chestek, P. S. Cederna, A regenerative peripheral nerve interface allows real-time control of an artificial hand in upper limb amputees. *Sci. Transl. Med.* **12**, eaay2857 (2020).
7. M. Ortiz-Catalan, B. Håkansson, R. Brånemark, An osseointegrated human-machine gateway for long-term sensory feedback and motor control of artificial limbs. *Sci. Transl. Med.* **6**, 257re6-257re6 (2014).
8. E. Mastinu, F. Clemente, P. Sassu, O. Aszmann, R. Brånemark, B. Håkansson, M. Controzzi, C. Cipriani, M. Ortiz-Catalan, Grip control and motor coordination with implanted and surface electrodes while grasping with an osseointegrated prosthetic hand. *J. Neuroeng. Rehabil.* **16**, 49 (2019).
9. M. Ortiz-Catalan, E. Mastinu, P. Sassu, O. Aszmann, R. Brånemark, Self-contained neuromusculoskeletal arm prostheses. *N. Engl. J. Med.* **382**, 1732–1738 (2020).
10. M. Ortiz-Catalan, R. Brånemark, B. Håkansson, J. Delbeke, On the viability of implantable electrodes for the natural control of artificial limbs: Review and discussion. *Biomed. Eng. Online* **11**, 33 (2012).
11. M. Ortiz-Catalan, J. Marin-Millan, J. Delbeke, B. Håkansson, R. Brånemark, Effect on signal-to-noise ratio of splitting the continuous contacts of cuff electrodes into smaller recording areas. *J. Neuroeng. Rehabil.* **10**, 22 (2013).
12. M. Ortiz-Catalan, R. Brånemark, B. Håkansson, BioPatRec: A modular research platform for the control of artificial limbs based on pattern recognition algorithms. *Source Code Biol. Med.* **8**, 11 (2013).
13. L. M. Hermansson, A. G. Fisher, B. Bernspång, A.-C. Eliasson, Assessment of capacity for myoelectric control: A new Rasch-built measure of prosthetic hand control. *J. Rehabil. Med.* **37**, 166–171 (2005).
14. E. Mastinu, R. Branemark, O. Aszmann, M. Ortiz-Catalan, in *Proceedings of the 2018 40th Annual International Conference of the IEEE Engineering in Medicine and Biology Society (EMBC)* (IEEE, 2018), vol. 2018-July, pp. 5174–5177.
15. L. E. Osborn, C. W. Moran, M. S. Johannes, E. E. Sutton, J. M. Wormley, C. Dohopolski, M. J. Nordstrom, J. A. Butkus, A. Chi, P. F. Pasquina, A. B. Cohen, B. A. Wester, M. S. Fifer, R. S. Armiger, Extended home use of an advanced osseointegrated prosthetic arm improves function, performance, and control efficiency. *J. Neural Eng.* **18**, 026020 (2021).
16. C. Cipriani, C. Antfolk, M. Controzzi, G. Lundborg, B. Rosen, M. C. Carrozza, F. Sebelius, Online myoelectric control of a dexterous hand prosthesis by transradial amputees. *IEEE Trans. Neural Syst. Rehabil. Eng.* **19**, 260–270 (2011).
17. E. M. Janssen, H. L. Benz, J. H. Tsai, J. F. P. Bridges, Identifying and prioritizing concerns associated with prosthetic devices for use in a benefit-risk assessment: A mixed-methods approach. *Expert Rev. Med. Devices* **15**, 385–398 (2018).
18. M. Ortiz-Catalan, B. Håkansson, R. Brånemark, Real-time and simultaneous control of artificial limbs based on pattern recognition algorithms. *IEEE Trans. Neural Syst. Rehabil. Eng.* **22**, 756–764 (2014).
19. H. Y. N. Lindner, A. Langius-Eklöf, L. M. N. Hermansson, Test-retest reliability and rater agreements of assessment of capacity for myoelectric control version 2.0. *J. Rehabil. Res. Dev.* **51**, 635–644 (2014).
20. A. Middleton, M. Ortiz-Catalan, Neuromusculoskeletal arm prostheses: Personal and social implications of living with an intimately integrated bionic arm. *Front. Neurorobot.* **14**, 39 (2020).
21. E. J. Earley, J. Zbinden, M. Munoz-Novoa, E. Mastinu, A. Smiles, M. Ortiz-Catalan, Competitive motivation increased home use and improved prosthesis self-perception after Cybathlon 2020 for neuromusculoskeletal prosthesis user. *J. Neuroeng. Rehabil.* **19**, 47 (2022).
22. D. Farina, I. Vujaklija, M. Sartori, T. Kapelner, F. Negro, N. Jiang, K. Bergmeister, A. Andalib, J. Principe, O. C. Aszmann, Man/machine interface based on the discharge timings of spinal motor neurons after targeted muscle reinnervation. *Nat. Biomed. Eng.* **1**, 0025 (2017).
23. S. Muceli, K. D. Bergmeister, K.-P. Hoffmann, M. Aman, I. Vukajlija, O. C. Aszmann, D. Farina, Decoding motor neuron activity from epimysial thin-film electrode recordings following targeted muscle reinnervation. *J. Neural Eng.* **16**, 016010 (2019).
24. J. A. George, T. S. Davis, M. R. Brinton, G. A. Clark, Intuitive neuromyoelectric control of a dexterous bionic arm using a modified Kalman filter. *J. Neurosci. Methods* **330**, 108462 (2020).
25. B. Ahkami, E. Mastinu, E. Earley, M. Ortiz-Catalan, Extra-neural signals from severed nerves enable intrinsic hand movements in transhumeral amputations. *Sci. Rep.* **12**, 10218 (2022).
26. K. Hagberg, E. Häggström, M. Uden, R. Brånemark, Socket versus bone-anchored transfemoral prostheses. *Prosthet. Orthot. Int.* **29**, 153–163 (2005).
27. H. Van de Meent, M. T. Hopman, J. P. Frölke, Walking ability and quality of life in subjects with transfemoral amputation: A comparison of osseointegration with socket prostheses. *Arch. Phys. Med. Rehabil.* **94**, 2174–2178 (2013).
28. A. Thesleff, E. Häggström, R. Tranberg, R. Zügner, A. Palmquist, M. Ortiz-Catalan, Loads at the implant-prosthesis interface during free and aided ambulation in osseointegrated transfemoral prostheses. *IEEE Trans. Med. Robot. Bionics* **2**, 497–505 (2020).
29. E. Mastinu, L. F. Engels, F. Clemente, M. Dione, P. Sassu, O. Aszmann, R. Brånemark, B. Håkansson, M. Controzzi, J. Wessberg, C. Cipriani, M. Ortiz-Catalan, Neural feedback strategies to improve grasping coordination in neuromusculoskeletal prostheses. *Sci. Rep.* **10**, 11793 (2020).
30. E. Mastinu, P. Doguet, Y. Botquin, B. Hakansson, M. Ortiz-Catalan, Embedded system for prosthetic control using implanted neuromuscular interfaces accessed via an osseointegrated implant. *IEEE Trans. Biomed. Circuits Syst.* **11**, 867–877 (2017).
31. B. Hudgins, P. Parker, R. N. Scott, A new strategy for multifunction myoelectric control. *I.E.E.E. Trans. Biomed. Eng.* **40**, 82–94 (1993).
32. C. M. Light, P. H. Chappell, P. J. Kyberd, Establishing a standardized clinical assessment tool of pathologic and prosthetic hand function: Normative data, reliability, and validity. *Arch. Phys. Med. Rehabil.* **83**, 776–783 (2002).
33. J. G. M. Burgerhof, E. Vasluian, P. U. Dijkstra, R. M. Bongers, C. K. van der Sluis, The southampton hand assessment procedure revisited: A transparent linear scoring system, applied to data of experienced prosthetic users. *J. Hand Ther.* **30**, 49–57 (2017).

Acknowledgments: We thank the individual who participated in this study and his family for their time and efforts. We thank D. M. Espinosa for preparing fig. S1. **Funding:** This study was supported by the Promobilia Foundation grant no. 19500 (to M.O.-C.), the IngaBritt and Arne Lundbergs Foundation grant no. 2018-0026 (to M.O.-C.), and the Swedish Research Council (Vetenskapsrådet) grant no. 2020-04817 (to M.O.-C.). **Author contributions:** M.O.-C., P.S., and R.B. conceived the surgical approach. M.O.-C. and R.B. developed the implant system. M.O.-C and E.M. developed the embedded prosthetic controller. P.S. and R.B. performed the surgeries. J.Z., E.M., E.J.E., and M.M.-N conducted the experiments. J.Z. analyzed the data. J.Z. and M.O.-C. drafted the manuscript. All authors revised and approved the final version of the manuscript. **Competing interests:** E.M. and M.O.-C. have consulted for Integrum AB. M.O.-C. and R.B. hold shares of Integrum AB. R.B. is the CEO of Integrum AB. M.O.-C. and R.B. are coinventors on patent no. US9579222B2 titled "Percutaneous gateway, a fixing system for a prosthesis, a fixture and connecting means for signal transmission," which is held by Integrum AB. The authors declare that they have no other competing interests. **Data and materials availability:** All data associated with this study are present in the paper or the Supplementary Materials.

Submitted 8 April 2022
Resubmitted 29 March 2023
Accepted 23 June 2023
Published 12 July 2023
10.1126/scitranslmed.abq3665

Science Translational Medicine

Improved control of a prosthetic limb by surgically creating electro-neuromuscular constructs with implanted electrodes

Jan Zbinden, Paolo Sassu, Enzo Mastinu, Eric J. Earley, Maria Munoz-Novoa, Rickard Brnemark, and Max Ortiz-Catalan

Sci. Transl. Med., **15** (704), eabq3665.
DOI: 10.1126/scitranslmed.abq3665

Science Translational Medicine (ISSN) is published by the American Association for the Advancement of Science. 1200 New York Avenue NW, Washington, DC 20005. The title *Science Translational Medicine* is a registered trademark of AAAS.